Optimizing RLS

Seiichi Tagawa

The Institute of Scientific and Industrial Research
Osaka University
and
JST-CREST

IEUVI Resist TWG
October 2, 2008

Acknowledgement

- Prof. Takahiro Kozawa
- Dr. Akinori Kozawa
- Dr. Hiroki Yamamoto
- Dr. Kazumasa Okamoto
- Mr. Ken-ichiro Natsuda
- Mr. Ryo Hirose
- Staffs and students in our Lab.
- Many co-workers in companies and research consortia

Saport form JST-CREST, Grant-in-Aid for Scientific Research, Selete, ASET, and Companies

RLS Trade Off:
The Most Crucial Issue in EUV Resist Development

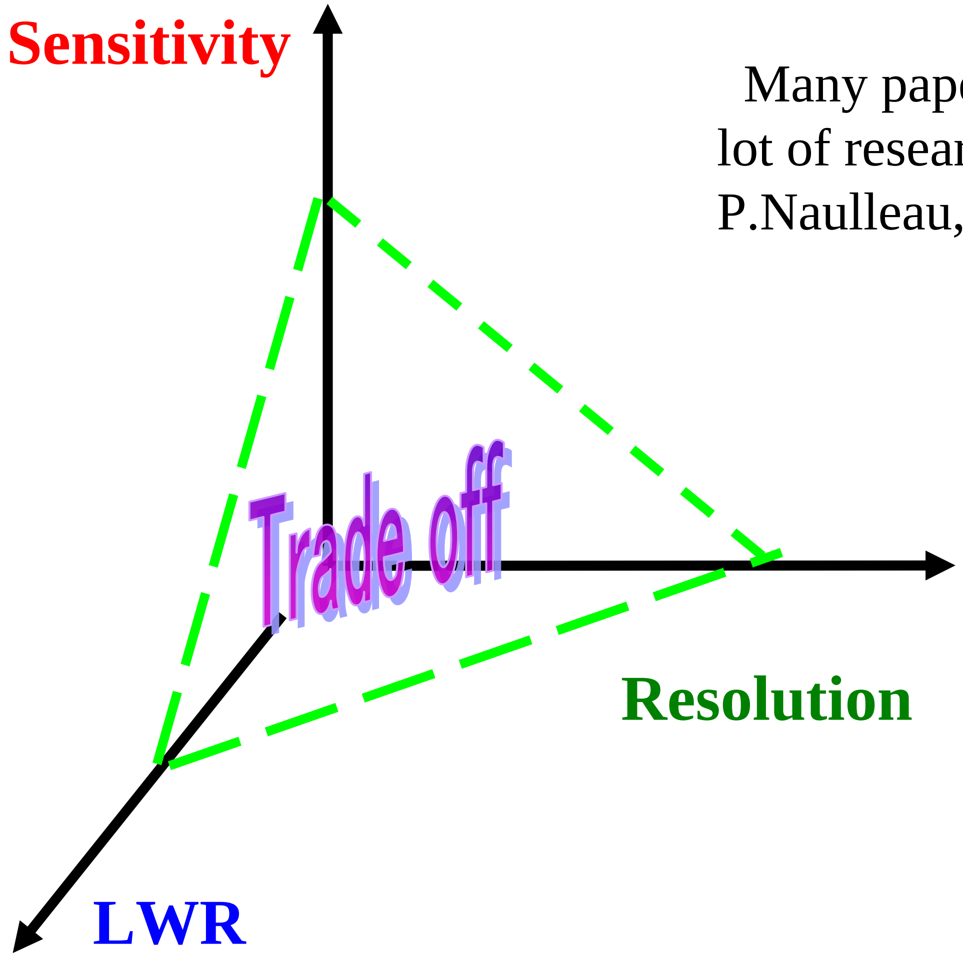

Many papers have been reported on RLS by a lot of researchers such as R.Brainard, T.Wallow, P.Naulleau, G.Gallatin, et al.

Experiments

R.Brainard et al. SPIE(2004)

P.Naulleau et al. SPIE(2006)

Simulations

G.M.Gallatin,SPIE(2005)

How to optimize RLS: Fundametal research is essential.

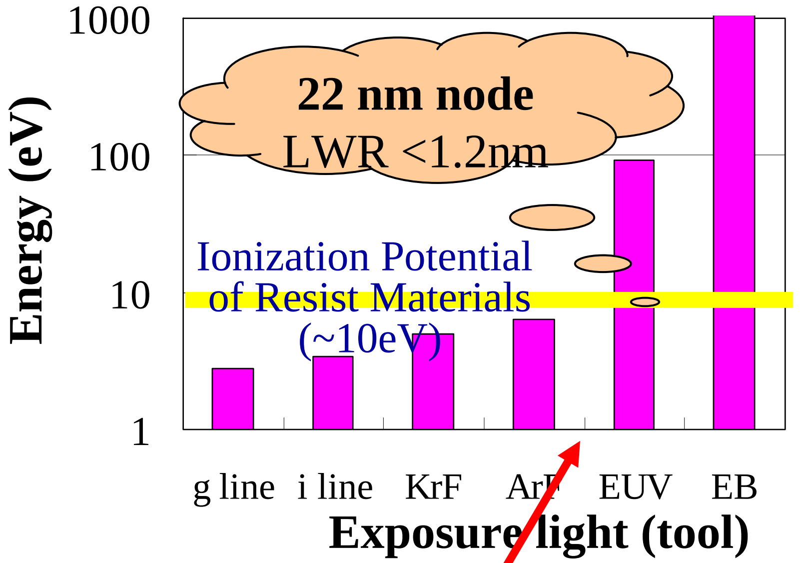

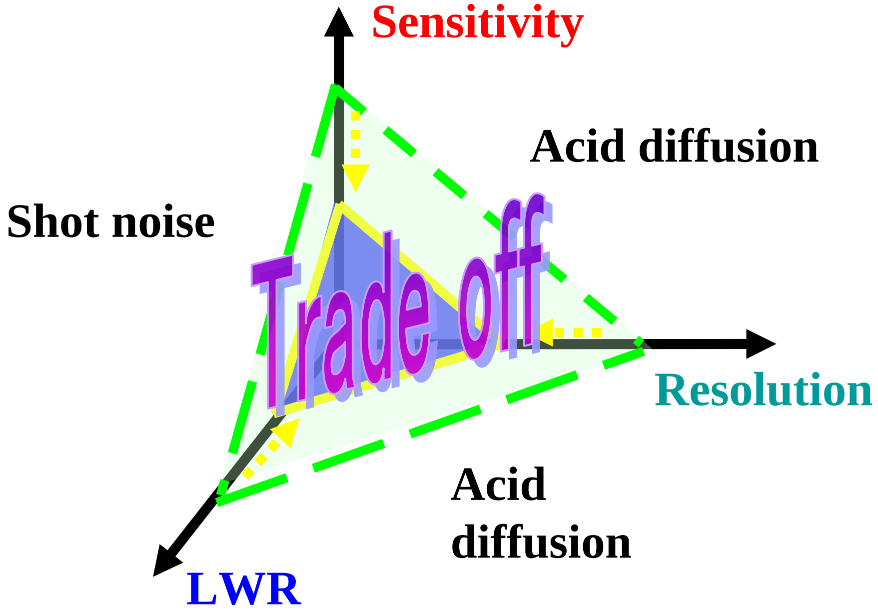

Huge amounts of knowledge infrastructure based on photochemstry are available for photoresists.

Solutions!

One of the best solution is the increase in pattern formation efficiency

New knowledge infrastructure based on radiation chemistry is essential for EUV resists.

Resist pattern formation processes

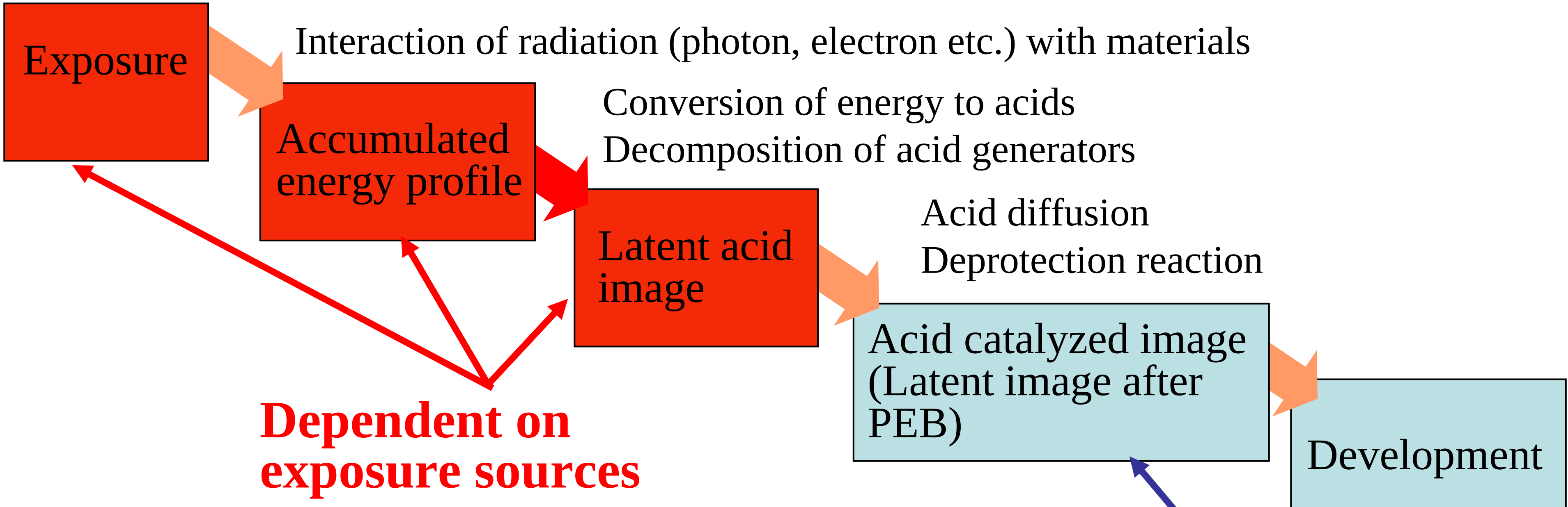

Exposure

Interaction of radiation (photon, electron etc.) with materials

Accumulated energy profile

Conversion of energy to acids
Decomposition of acid generators

Latent acid image

Acid diffusion
Deprotection reaction

Acid catalyzed image (Latent image after PEB)

Development

Dependent on exposure sources

Independent of exposure sources

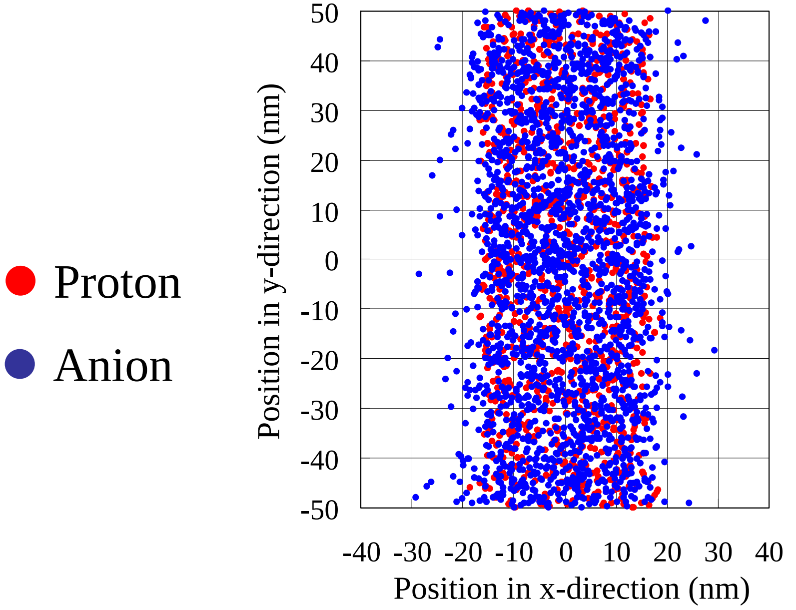

Proton-anion distribution

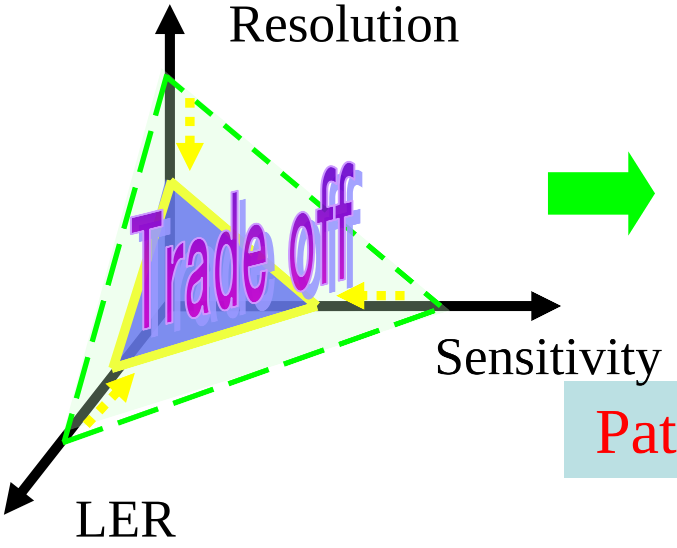

The increase in pattern formation efficiency is required to simultaneously meet the requirements for RLS.

Pattern formation efficiency

||

Absorption efficiency of incident energy
(mainly absorption coefficient of polymer)

Exposure source dependent

X

Limited by side wall degradation

Quantum yield of acid

X

Limited by secondary electron emission efficiency

Exposure source independent

Efficiency of catalytic chain reaction

Limited by diffusion-controlled rate for chemical reaction

Other factors:Initial distribution of acid in nanospace and development etc..

Important point of diffusion length（$\sqrt{2Dt}$）and pattern size

It has been believed that a resist with an acid diffusion length of, for example, 15 nm cannot resolve 22 nm patterns. However, this is not true in the presence of quenchers. The resolution does not necessarily depend on the acid diffusion length. Pattern sizes are determined by a initial distribution of acids and quenchers, and ratio between the acid and quencher diffusion constants. (Jpn. J. Appl. Phys. 47 (2008) 4465, 4926, 5404)

The concept of recent quencher controlled CAR is different from classical CAR.

Acid diffusion and chemical reaction

Acid diffusion and reaction

$$\frac{\partial u_{acid}}{\partial t} = \nabla\left(D_{acid}\nabla u_{acid}\right) - k u_{acid} u_{quencher}$$

Base quencher diffusion and reaction

$$\frac{\partial u_{quencher}}{\partial t} = \nabla\left(D_{quencher}\nabla u_{quencher}\right) - k u_{acid} u_{quencher}$$

Deprotection reaction, especially rate constant

$$[P] = -\int_0^{T_{PEB}} k_{depro} u_{acid} [P] dt$$

Optimization of quencher concentration for each α

It has been reported that quenchers affect RLS. However the details are still unclear.

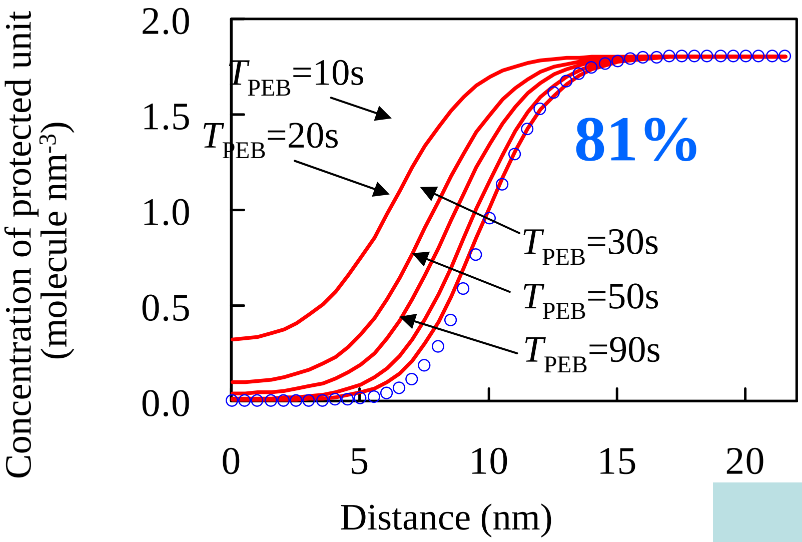

(a) α = 0.1

$$\alpha = \frac{D_{quencher}}{D_{acid}}$$

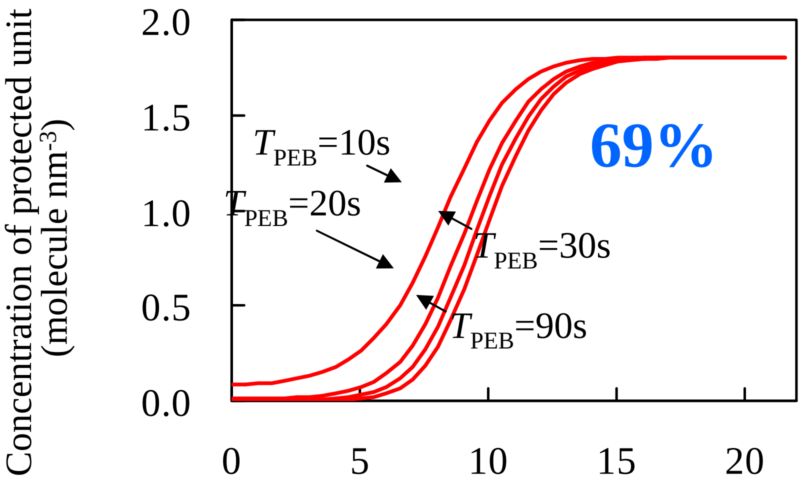

Distance (nm)

(b) α = 1

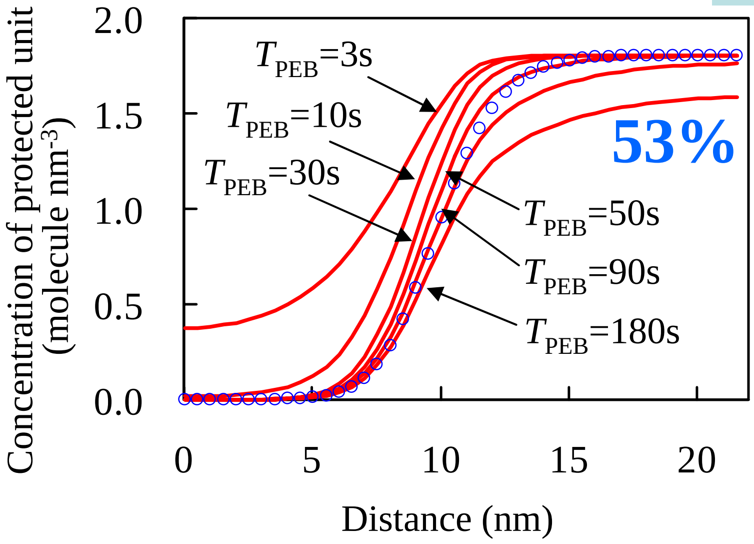

(c) α = 10

Fig. Temporal changes of latent images during PEB. The exposure dose is 20 mJ cm^{-2}. The quencher concentrations are (a) 81%, (b) 69%, and (c) 53% of initial acid concentration at the origin. The open circles represent the same deprotection profile as the one at T_{PEB} = 90 s in Fig. (b).

Conclusion: the same order of diffusion costants for acids and quenchers are preferable for 22 nm fabrication

Jpn. J. Appl. Phys. 47 (2008) 5404.

Limit of PHS-based chemically amplified resist

Jpn. J. Appl. Phys. 47 (2008) 4465.

Latent images of 22 nm line & space

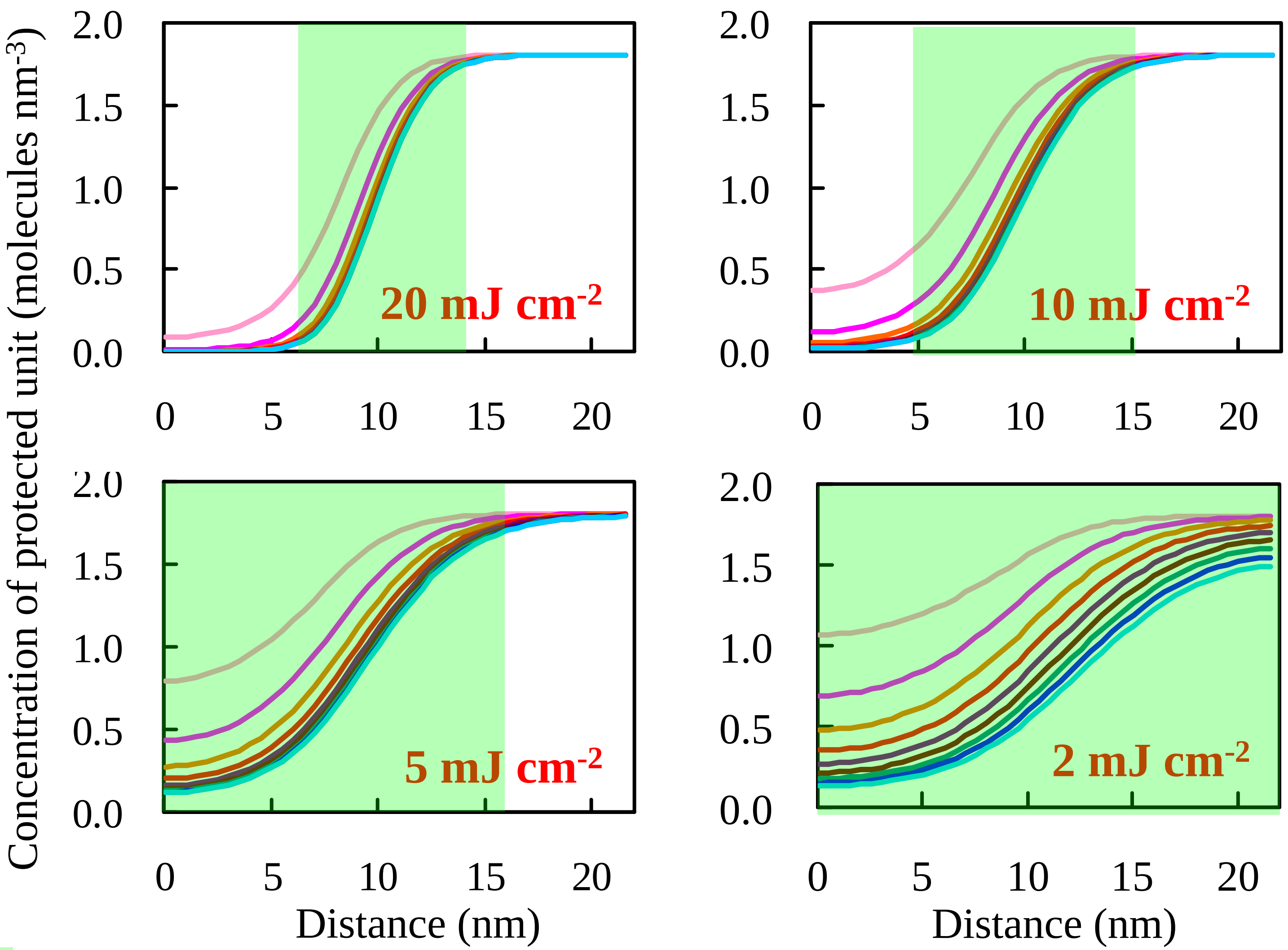

🟩 Intermediate region where protected and deprotected units coexist

The width expands with $1/\sqrt{dose}$ dependence.

Conclusion of the increase in pattern formation by opimizing the catalytic chain reactions

When only the catylitic chain reactions are controled, 22 nm fabrication is achievable with 10 mJ cm-2 exposure dose and a high quality image is unlikely to be obtained with 5 mJ cm^{-2} exposure dose without some special consideration of the catalytic chain reactions and increases in acid generation efficiency and polymer absorption.

Some special consideration such as anisotropic acid diffusion (Gallatin, Naulleau, Brainard SPIE(2007)) and nonconstant diffusion coefficient. (T. Kozawa et al., J. Photopoly.Sci.Tech., 21(2008)421)

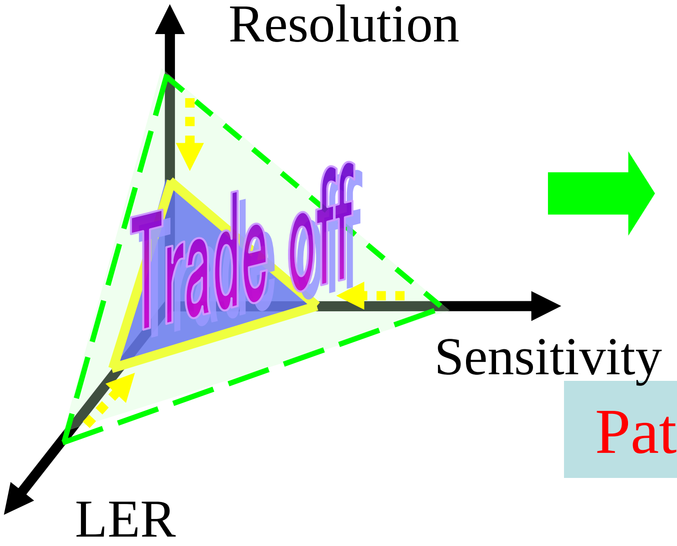

The increase in pattern formation efficiency is required to simultaneously meet the requirements for RLS.

Pattern formation efficiency

||

Absorption efficiency of incident energy (mainly absorption coefficient of polymer)

Limited by side wall degradation

X

Quantum yield of acid

Limited by secondary electron emission efficiency

X

Efficiency of catalytic chain reaction

Limited by diffusion-controlled rate for chemical reaction

Exposure source dependent

Exposure source independent

Other factors:Initial distribution of acid in nanospace and development etc..

Acid Generation of Chemically Amplified EUV Resists

EUV： Main reactions start from ionizatin of polymer.

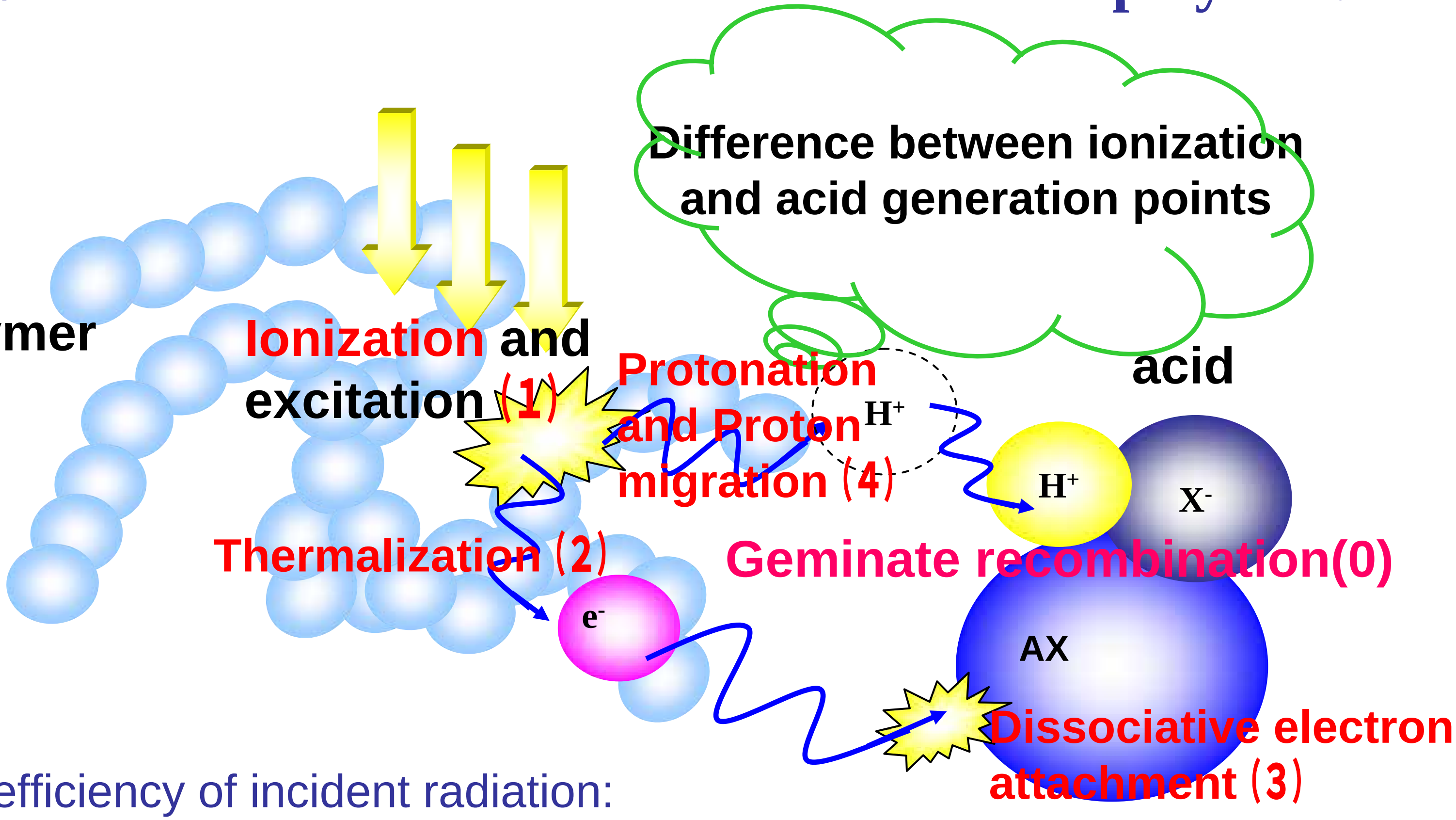

Difference between ionization and acid generation points

polymer

Ionization and excitation (1)

Protonation and Proton migration (4)

acid

Geminate recombination(0)

Thermalization (2)

Dissociative electron attachment (3)

Absorption efficiency of incident radiation:

absorption coefficient α, ultra thin film(multi-layer resist)

Quantum yield of acid:

concentration of acid generator, dielectric constants, acid amplification, proton formation and transport, counter anion generation efficiency, etc. (Many papers by us)

Nanospace control of acid generation:

reaction of epithermal electrons (K. Natsuda et al. J.J.Appl.Phys., 47(2008)4932)

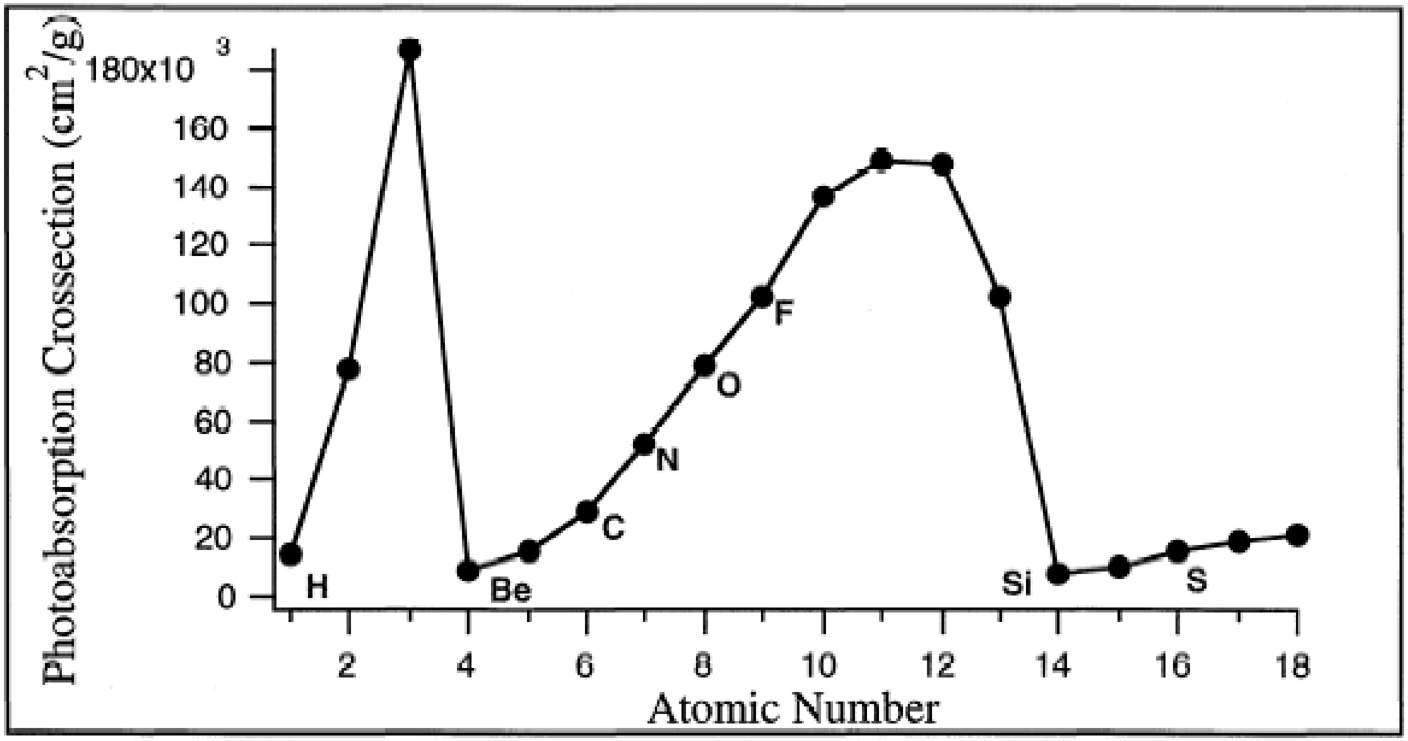

Figure 1: Elemental absorption cross-sections at 13.4 nm wavelength. Elements commonly found in photoresist materials are H, C, N, O, F, and S.

P. Dentinger et al., SPIE 3997 (2000) 588.

Interaction of EUV photon with CARs -spatial distribution-

Intensity of EUV (I)

$$\boxed{\frac{\partial I}{\partial z} = -\alpha I}$$

Absorption coefficient (**α**)

PHS : 3.8 μm^{-1}

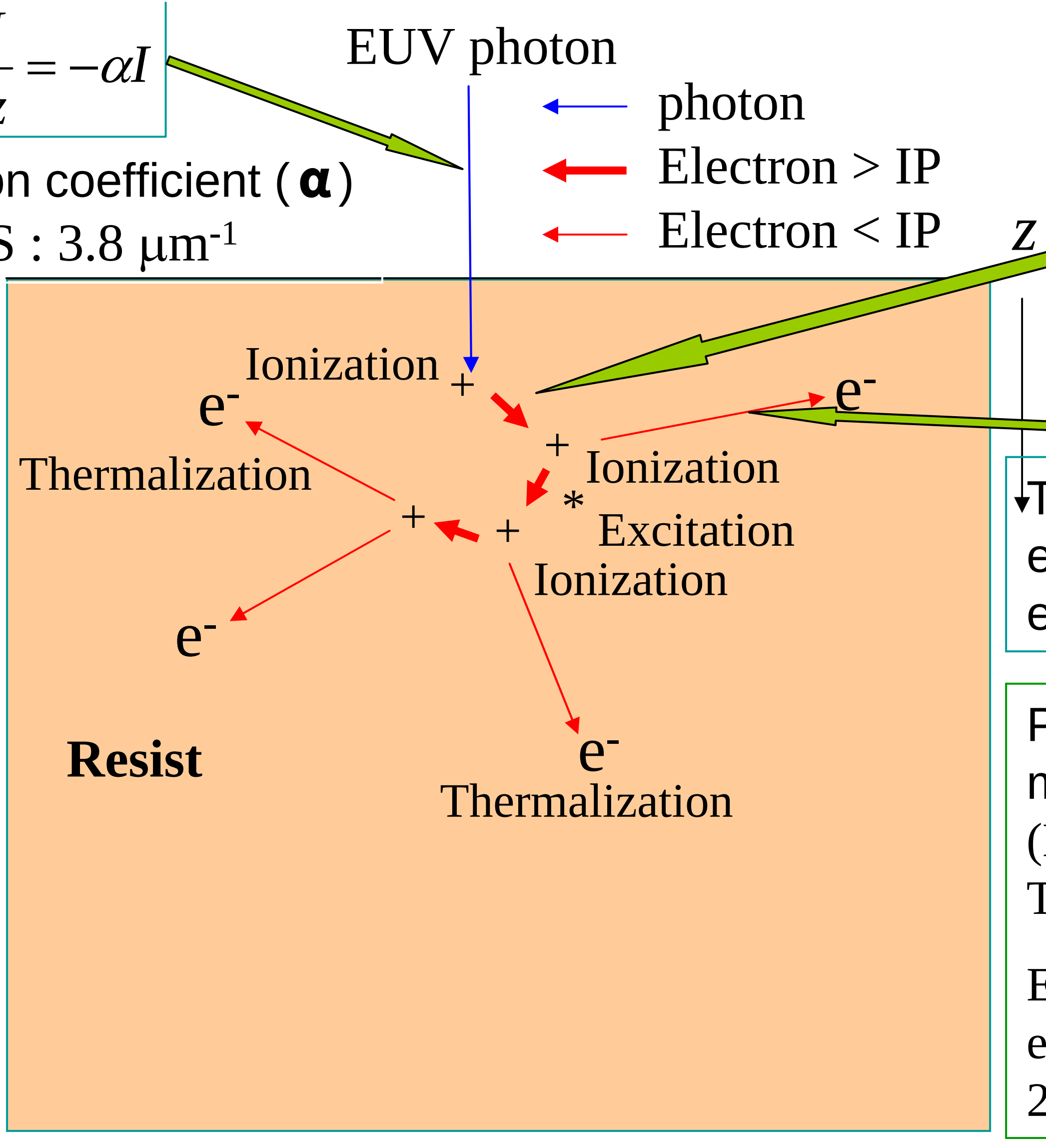

Inelastic mean free path

<1 nm mean free path at electron with energy > IP

Thermalization Length 4.0 nm for PHS

The number of secondary electrons is estimated expermentally. 4.2 for PHS

PHS with 10 wt% TPS-tf Acid molecules per photon: 2.6 (Kozawa et al. J.Vac.Sci. Tecnnol.,B25(2007) 2481)

Experimental value: 2.5 (Hirose et al.,Jap.J.Appl.Phys,Part 2(2007)

Difference between EB and EUV

EB

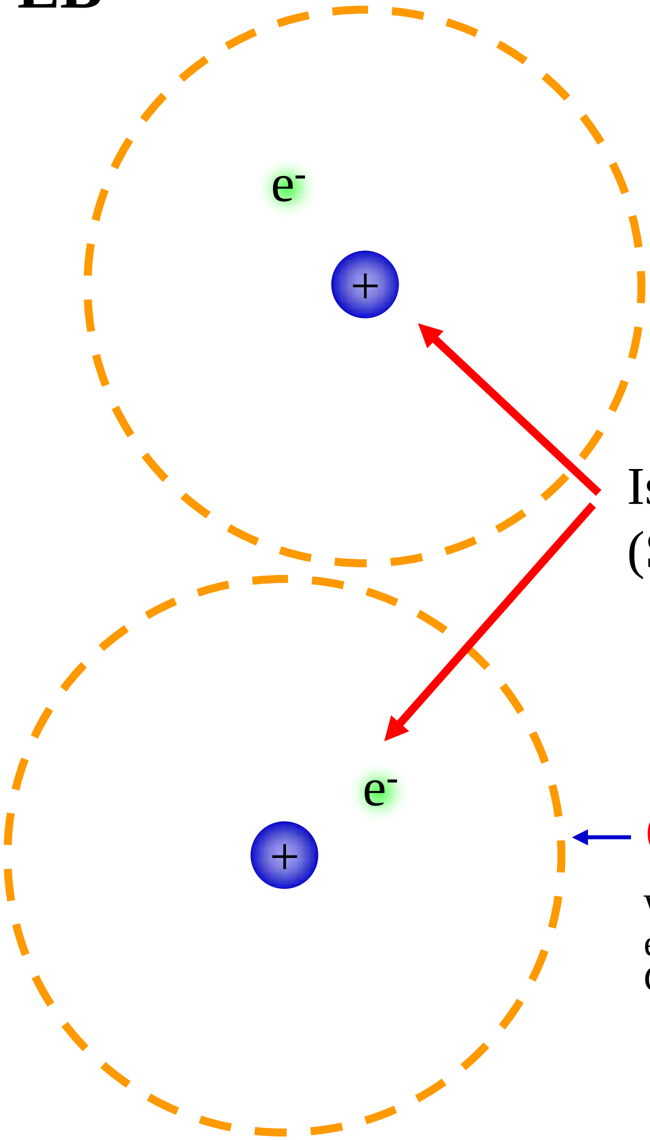

Isolated pairs
(Single spur)

Onsager distance

Where the thermal energy of electron correspond to the Coulomb potential.

$$r_c = \frac{e^2}{\varepsilon kT}$$

～14 nm
in PHS

EUV

Multi spur effect

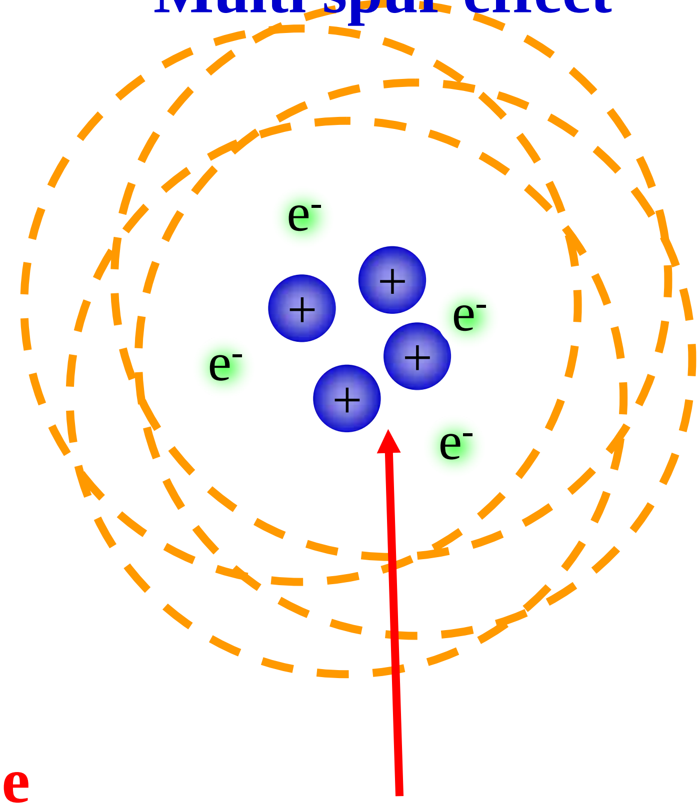

Stronger electric field

(Kozawa et al., J.Appl.Phys, 103(2008)84306)

Electron dynamics in early processes of radiation chemistry

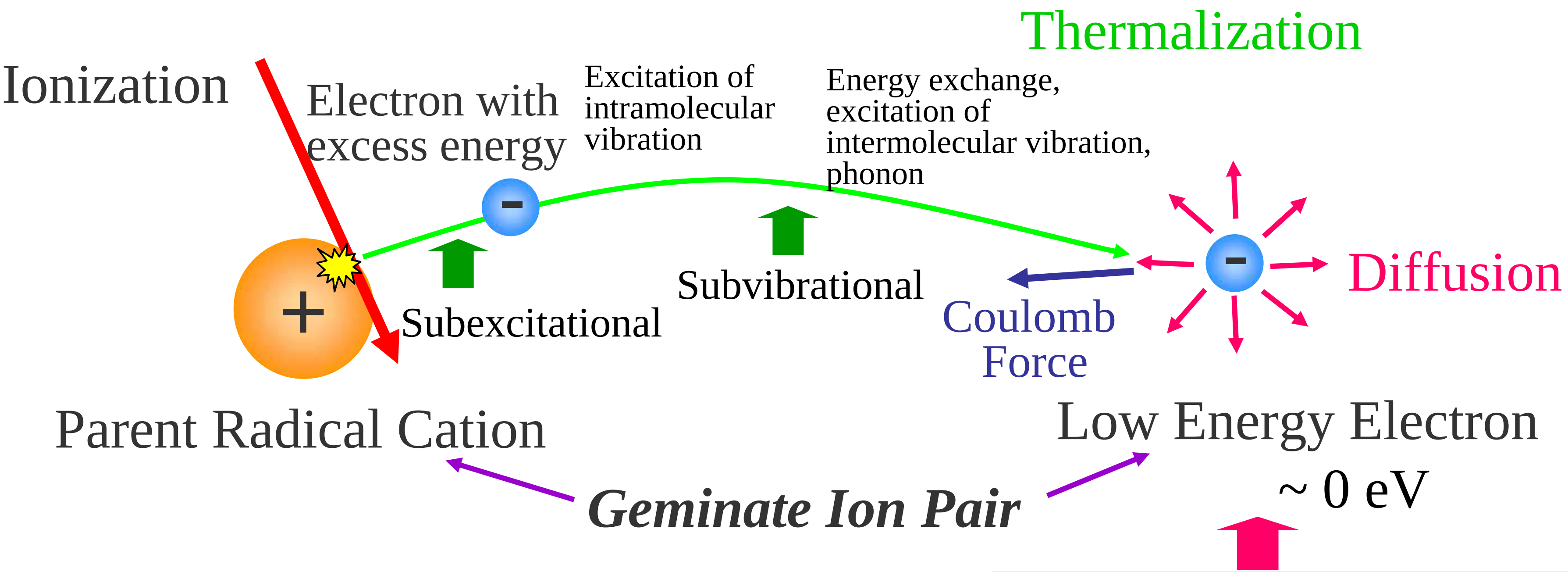

Thermalization

Ionization

Electron with excess energy

Excitation of intramolecular vibration

Energy exchange, excitation of intermolecular vibration, phonon

Subexcitational

Subvibrational

Coulomb Force

Diffusion

Parent Radical Cation

Low Energy Electron

~ 0 eV

Geminate Ion Pair

Acid generator can react with these low energy electrons.

Modified Smoluchowski equation for CAR

$$\frac{\partial w}{\partial Dt} = \nabla\left(\nabla w + w\frac{1}{k_B T}\nabla V\right) - 4\pi RCw$$

w : Probability density of electrons

k_B : Boltzmann constant

V : Coulomb potential(Dielectric constant)

T : Absolute temperature

D : Sum of diffusion coefficient

C : concentration of acid generators

R : effective reaction radius

Initial distribution function

$$f(r, r_0) = \frac{1}{r_0}\exp\left(-\frac{r}{r_0}\right)$$

r : Distance between radical cation and electron

r_0 : Thermalization distance

Difference in sensitization distance between EUV and EB

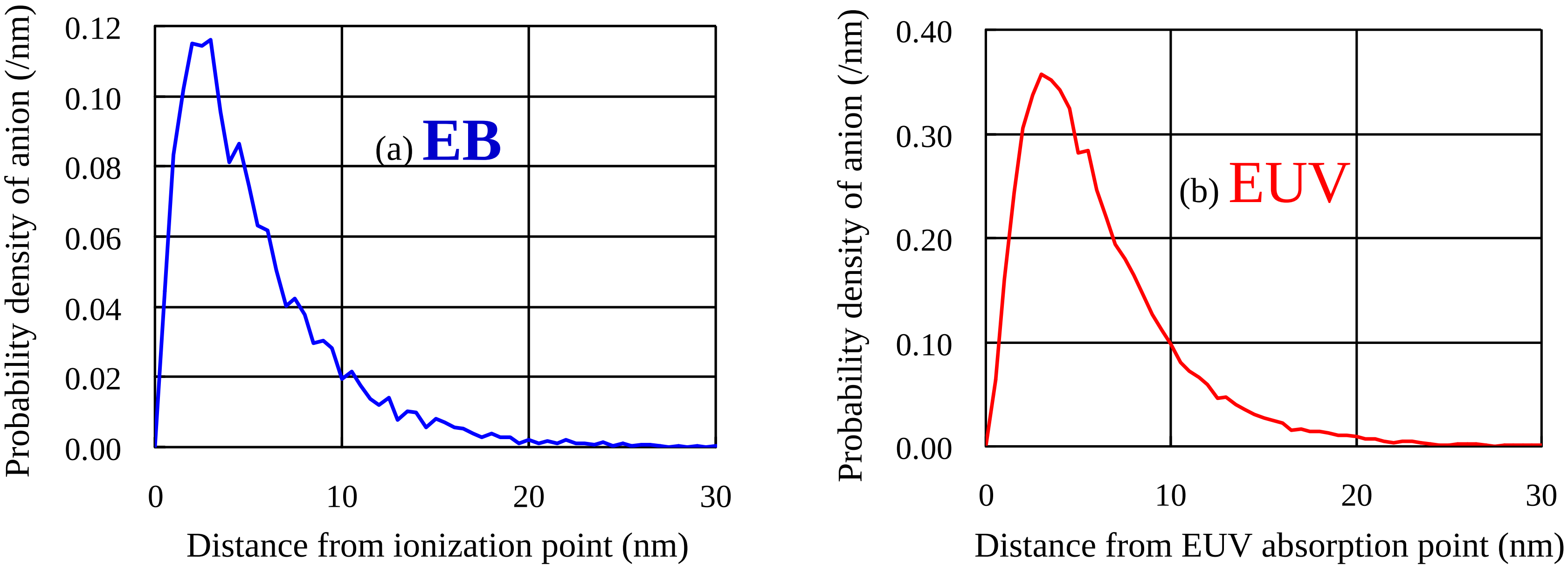

Fig. Probability density of anion generated in PHS with 10 wt% TPS-tf by (a) an electron and (b) an EUV photon.

Sensitization distance (ionization)

5.6 nm

6.3 nm

Acid generation efficiency (ionization)

0.74 per ionization

0.62 per ionization

G(acid) = 3.3 (3.3 acids per 100 eV)

2.6 acids per one photon(92.5 eV) in PHS

Kozawa and Tagawa, J.Vac.Sci.Tecnnol.,B25(2007) 2481

Kozawa et al. J.Vac.Sci.Tecnnol. B24,3055(2006)

Experimental value: 2.5 Hirose et al., Jap.J.Appl. Phys, Part 2 Let. & Express Let.,46,L979(2007)

Feasibility on High-Sensitivity Chemically Amplified Resist by Polymer Absorption Enhancement

(Appl. Phys. Express 1(2008)47001, 67012)

Current status

Sensitivity： 10~20 mJ cm^{-2}

Abs. coefficient： 3.8 μm^{-1} (PHS)

Thickness：50 nm (40-75 nm)

Transparency： 83%

X 1/4

Sensitivity： <5 mJ cm^{-2}

Abs. coefficient： 16 μm^{-1}

Thickness：20 nm

Transparency： 73%

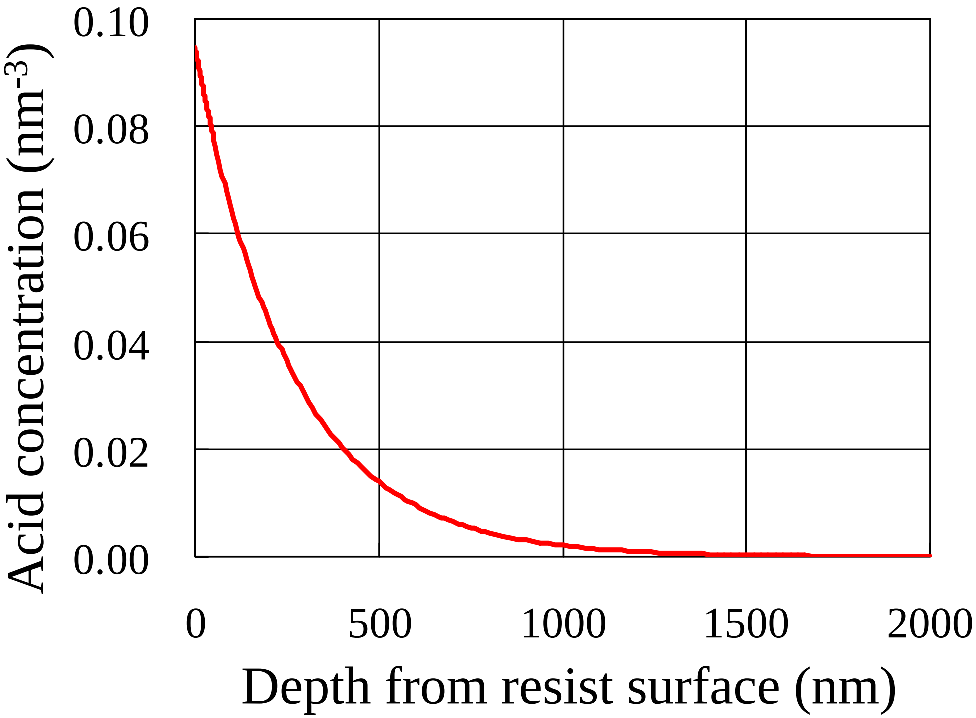

Depth profile

Fig. Depth profile of acid concentration (The number of acid molecules per unit volume). The exposure dose is 10 mJ cm^{-2}.

side wall degradation

Reinvestigation is necessary for the relationship between absorption coefficient and side wall angle because of the difference in the sensitization mechanisms of DUV and EUV resists.

We studied the feasibility of high absorption resist process using a simulation from the viewpoint of side wall degradation

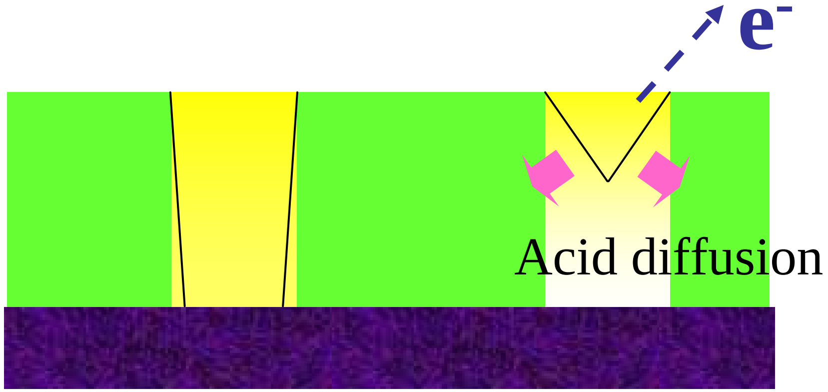

Acid distribution is determined by absorption coefficient.

Moderation through acid diffusion

Restriction in acid diffusion + Effect of secondary electrons

Electron emission from surface

Electron emission depends on work function of materials, W_f.

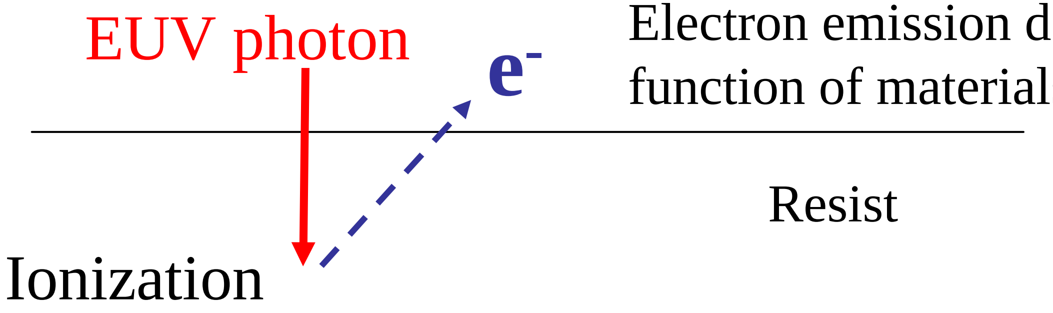

Total-reflection model：$W_f = \infty$ Total-transmission model：$W_f = 0$

22 nm L&S image formed in high absorption resist upon 5 mJ cm^{-2} exposure

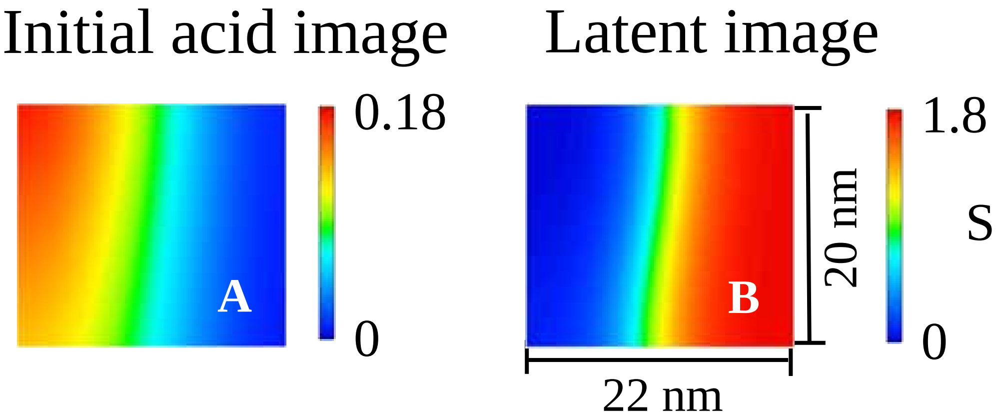

Side wall angle： 84.5 °

(a) Total-reflection model

Side wall angle： 89.4 °

(b) Total-transmission model

Two-dimensional initial acid distribution (A) and latent image (B) of 22 nm line-and-space patterns, calculated using a = 16 μm^{-1} with (a) total reflection and (b) total transmission models. The film thickness is 20 nm. The exposure dose is 5 mJ cm^{-2}. The quencher concentration is optimized to be 55% of the initial average acid yield in an area with the peak EUV intensity.

Conclusion: Compared with PHS-based resists, the fourfold enhancement of polymer absorption is feasible without side wall degradation partly due to the long migration range of secondary electrons, although it is necessary to reduce the resist thickness from 50 to 20 nm.

Conclusion

- To optimize RLS, the improvement of pattern formation efficiency is essential. The efficiency of pattern formation is mainly determined by three factors such as the absorption efficiency of incident radiation, quantum yield of acid, and efficiency of the catalytic chain reactions.
- When only the catalytic chain reactions are controled, 22 nm fabrication is achievable with 10 mJ cm-2 exposure dose and a high quality image is unlikely to be obtained with 5 mJ cm-2 exposure dose without some special consideration of the catalytic chain reactions and increases in acid generation efficiency and polymer absorption.
- Compared with PHS-based resists, the fourfold enhancement of polymer absorption is feasible without side wall degradation partly due to the long migration range of secondary electrons, although it is necessary to reduce the resist thickness from 50 to 20 nm.
- How to increase the quantum yield of acid is tightly connected with EUV resist reactions and we have published many papers in this field. The most effective method in this part is increasing in acid generator concentration, but we didn’t talk about it because of time limitation.
- Resist makers started the improvement of EUV resists based on above concept. The good improvement on RLS has been achieved recently.
- The fundamental concept of optimizing RLS is made clear, however, there are many remaining problems to optimize RLS.